



Geophysical contribution to evaluate the subsurface structural setting using magnetic and geothermal data in El-Bahariya Oasis, Western Desert, Egypt

Esmat Abd El All, Ahmed Khalil *, Taha Rabeh, Salah Osman

National Research Institute of Astronomy and Geophysics (NRIAG), 11722 Helwan, Cairo, Egypt

Received 30 December 2014; revised 17 August 2015; accepted 14 September 2015
Available online 3 October 2015

KEYWORDS

Magnetic;
Geothermal;
Euler deconvolution;
El Bahariya Oasis

Abstract The future development of agriculture, industry, and civil activity is planned to be in the Western Desert, Egypt. El-Bahariya Oasis is located in the heart of the Western Desert at a distance of about 370 km to the southwest of Cairo. The area under investigation is located between latitudes 28°06'N & 28°16'N and longitudes 28°54'E & 29°04'. The Bahariya depression comprises a total area of approximately 2250 km². The main target of the present study is to delineate the shallow and deep subsurface structures of the study area. To achieve this, two geophysical methods (magnetic and geothermal) have been used. A detailed land magnetic survey has been acquired. Fifty three land magnetic stations have been measured in a mesh like area with 500 m spacing interval. The necessary corrections concerning daily variation, the regional gradient and time variations have been applied. Then, the total magnetic intensity anomaly map (TMI) has been constructed and reduced to the pole magnetic map (RTP). The Euler deconvolution has been applied to the TMI anomaly data as well as the analytical signal technique. Also, the magnetic interpretation has been carried out using the high-pass filtering technique and spectral frequency analysis. The analysis of the magnetic data shows that the dominant tectonic trends are NW–SE and E–W. The results show that, the average calculated depth ranges between 0.1 km and 0.32 km, while the depth to the basement intrusion is 0.4 km, below the measuring level.

The geothermal studies in EL Bahariya-Oasis comprise subsurface temperature contour map which illustrates that the study area has geothermal groundwater reservoirs. The measurements of the geothermal properties for measured rock samples show that the rocks of the study area have moderate values of geothermal properties. This may be due to the seasonal variation in soil temperatures. These soil thermal properties depend on soil porosity and moisture content.

© 2015 Production and hosting by Elsevier B.V. on behalf of National Research Institute of Astronomy and Geophysics.

* Corresponding author.

E-mail address: ahmedbkr73@hotmail.com (A. Khalil).

Peer review under responsibility of National Research Institute of Astronomy and Geophysics.



Production and hosting by Elsevier

1. Introduction

The Western Desert covers the west of the Nile River and extends to the border with Libya. A number of diverse basins and structural features make up this province. The Bahariya Oasis is a large oval shaped NE-oriented depression located

in the north-central part of Western Desert of Egypt (Fig. 1). The Bahariya depression comprises a total area of approximately 2250 km² and is one of the five large oases in the Western Desert. The area falls under the arid condition as the total rainfall ranges from 3 to 6 mm/year. Springs and wells are the main two-groundwater resources for irrigation and civic purposes (Salem, 1987). Egypt is facing greatly increasing demands for water due to a rapidly growing population. Surface water resources originating from the Nile are now fully exploited (Hvidt, 1999). Recently, there has been a development program of progressive reclamation and urbanization of the desert including the investigated northern Bahariya Oasis. The main objective for this study is to delineate the shallow and deep subsurface structures of the studied area. To achieve this target, two geophysical methods are used (magnetic and geothermal investigations).

1.1. Geology of EL-Bahariya Oasis

The Bahariya Oasis is a large Syrian Arc age (Upper Cretaceous through late Eocene) anticline that forms the southern termination of the basins of the Western Desert. Upper Cretaceous reservoirs of the Bahariya Formation are well exposed,

as are some of the transpersonal structural features typical of the Syrian Arc orogenic event (Said, 1962). Oligocene basalts unconformably overlie the Bahariya Formation over most of the oasis. The oasis was an exposed landmass from Paleocene through Eocene time, when carbonate and anoxic lagoonal shale deposition dominated in the flanking lows. The Bahariya is a large natural excavation, surrounded by escarpments and has a large number of isolated hills within the depression. The general shape of the depression is oval with its major axis running northeast and with a narrow blunt-pointed extension at each end. The most striking features in the topography of the Bahariya Oasis are large number of hills within the depression (Said, 1962). Small separate parts of the depression are occupied by local people, while the rest are uninhabited. More than 100 flowing springs and 21 deep drilled wells are developed in the Bahariya depression. The regional section shown in Fig. 2 illustrates major differences between the Western Desert and the Nile Delta. Eocene and Oligocene strata seal the Western Desert petroleum system. At Bahariya Oasis, the stratigraphic section is dominantly clastic, reflecting proximity to Upper Egypt highlands that have long shed sediment northward into the Western Desert and Nile Delta. All sequences become sandy southward toward these highlands.

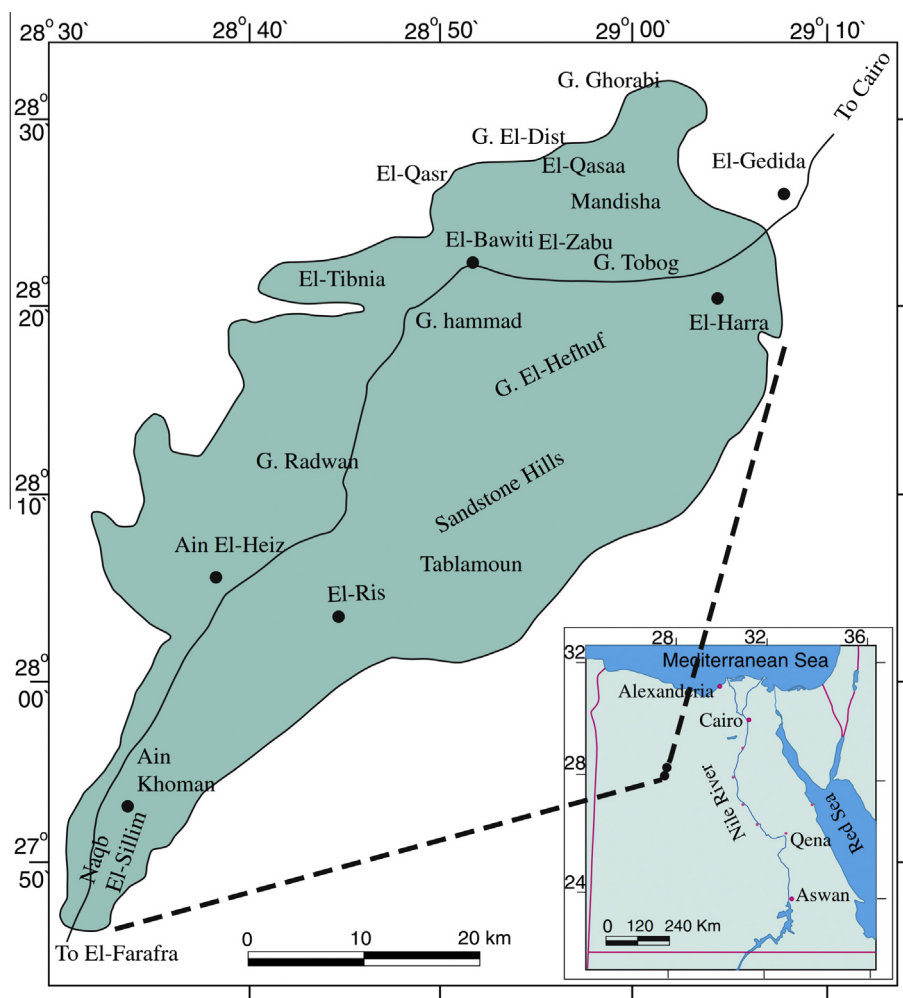


Figure 1 Location map of the El-Bahariya Oasis area.

Northward, numerous transgressive shales or marine carbonates allow subdivision of strata into major sequences and formations.

The lower Cenomanian (Bahariya Formation) displays in the main aquifer in this area. It is formed of successive layers of sandstone water-bearing layers of about 18–34 m in the thickness (Korany, 1981).

1.2. Geological structure of EL-Bahariya Oasis

The study area is highly deformed. Two periods of deformation affected the Bahariya Oasis. The upper Cretaceous section was deformed by the Laramide cycle, while the Eocene and Oligocene sediments were deformed by the Alpine cycle. Several folding and faulting systems are distinguished (Said, 1962; El-Atre and Moustafa, 1980). The Bahariya depression is built up of a great plugging anticline running (SW–NE). Two lines of minor folds are developed along the east and west sides of the major anticline.

Three fault systems are distinguished in Bahariya Oasis, (NE–SW) trending fault system with throw ranges between 40 and 174 ms, another (NW–SE) trending fault system with a throw ranges between 30 and 40 ms, and a third (E–W) trending fault system with a variable throw (Korany, 1984).

2. Magnetic data

2.1. Magnetic data acquisition

Since the magnetic method of prospecting gives an effective presentation of the subsurface structures, thus a detailed

land magnetic survey has been carried out for the total component of geomagnetic field. The measurements have been carried out using two Geometrics G-856 portable proton magnetometers with a 1 nT sensitivity. One instrument is used as a base station for the diurnal correction and the other is used to measure the magnetic field along the study area. The distances between the stations range from 400 to 500 m, depending on the topography (Fig. 3). The necessary corrections for the measured magnetic data have been achieved.

2.2. Processing and interpretation of magnetic data

The processing of the total intensity magnetic map (Fig. 4) is started by reduction to the magnetic north (RTP) in order to overcome the undesired distortion of the shapes, sizes and locations of the magnetic anomalies in which the RTP magnetic map is separated into residual and regional components. Their filters, regional and residual filters have been used in the interpretation and delineation of shallow and deep subsurface structures of the studied area. The quantitative interpretation has been used to determine the depths of shallow subsurface structures (faults and dykes), basaltic intrusions, as well as the basement complex of the considered area. The methods of interpretations are the radially averaged power spectrum, Euler deconvolution and analytical signal. The processing and analysis have been done by specialized computer software (Oasis Montaj (1998)). The resulting RTP land magnetic map (Fig. 5) shows the direct correlation between the magnetic anomalies and their causative sources. An average magnetic

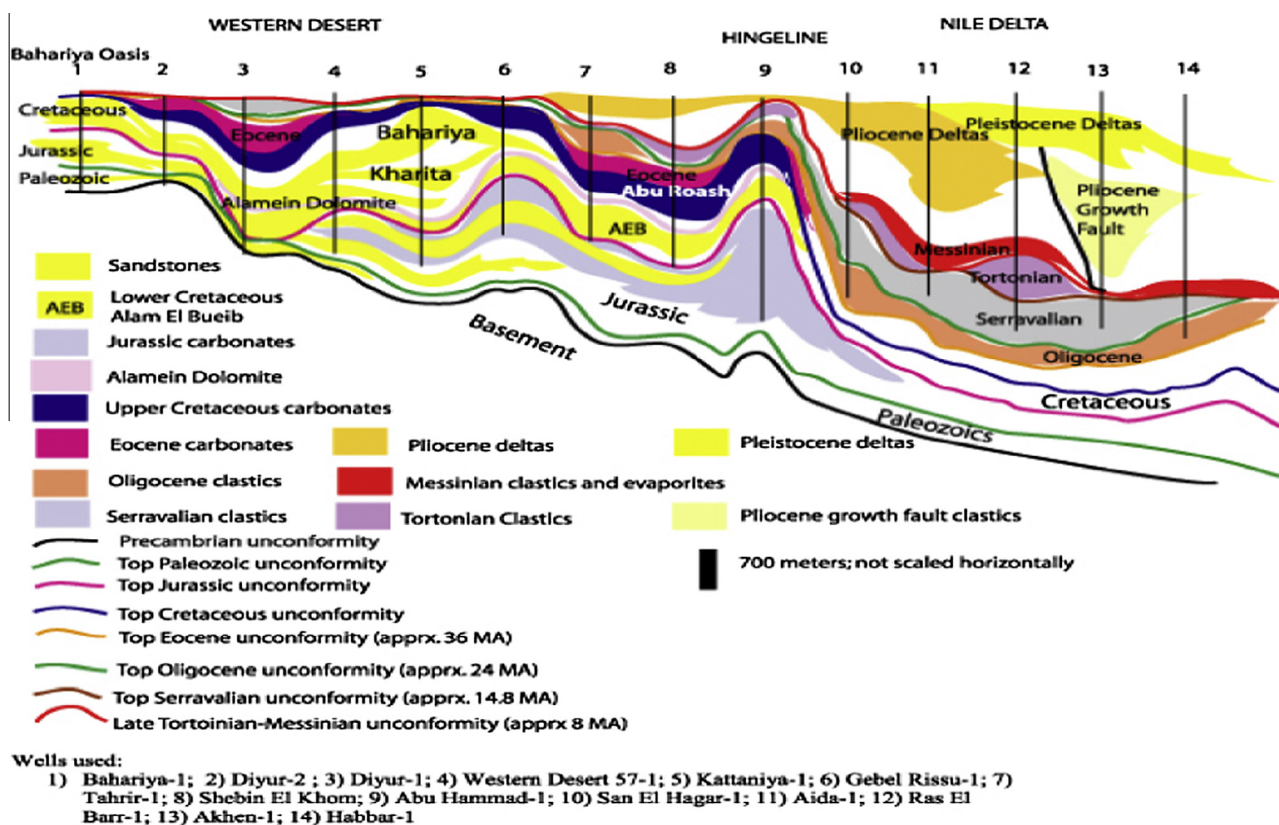


Figure 2 Regional cross-section (not scaled) from El-Bahariya Oasis to the Nile Delta (El Sisi et al., 2002).

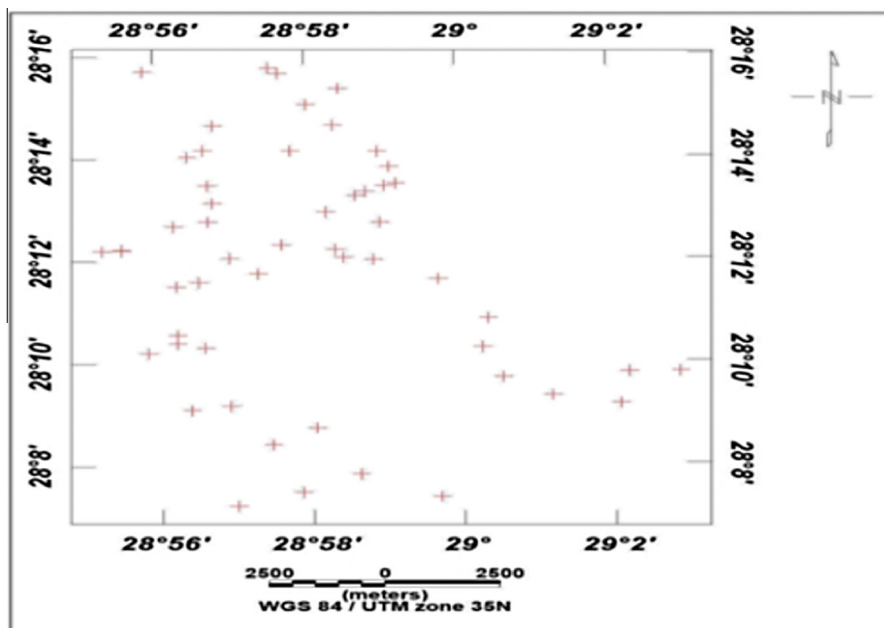


Figure 3 Location map of the land magnetic survey stations.

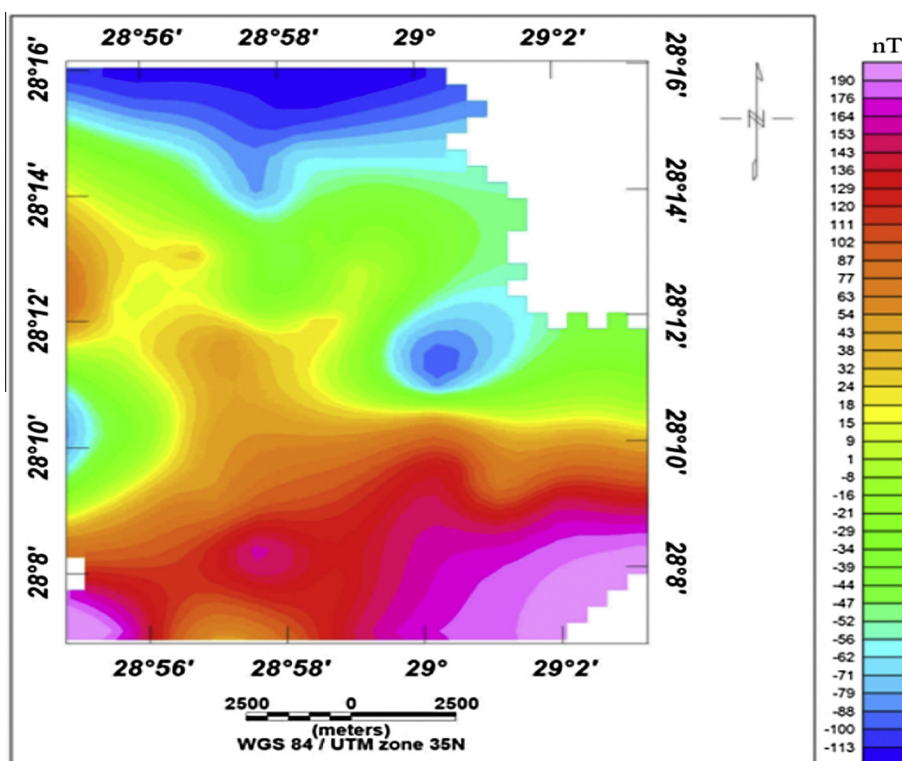


Figure 4 Total intensity magnetic anomaly map for the study area.

inclination of 42° is used for the studied area, to eliminate the obliquity of the inclination of the earth's magnetic field.

2.3. Structural indications of the RTP land magnetic map

From the inspection of land magnetic intensity map (Fig. 4), we notice that, there are local magnetic anomalies superimposed

on the regional magnetic field. These anomalies are most probably related to basement faulting structures. Some zones of high contour-line densities, which indicate high horizontal magnetic gradients, could be interpreted as locations of fault planes. The major local anomalies are located between high and low magnetic anomalies that show locations of probable fault planes. The Reduced-To-Pole magnetic map (Fig. 5) is

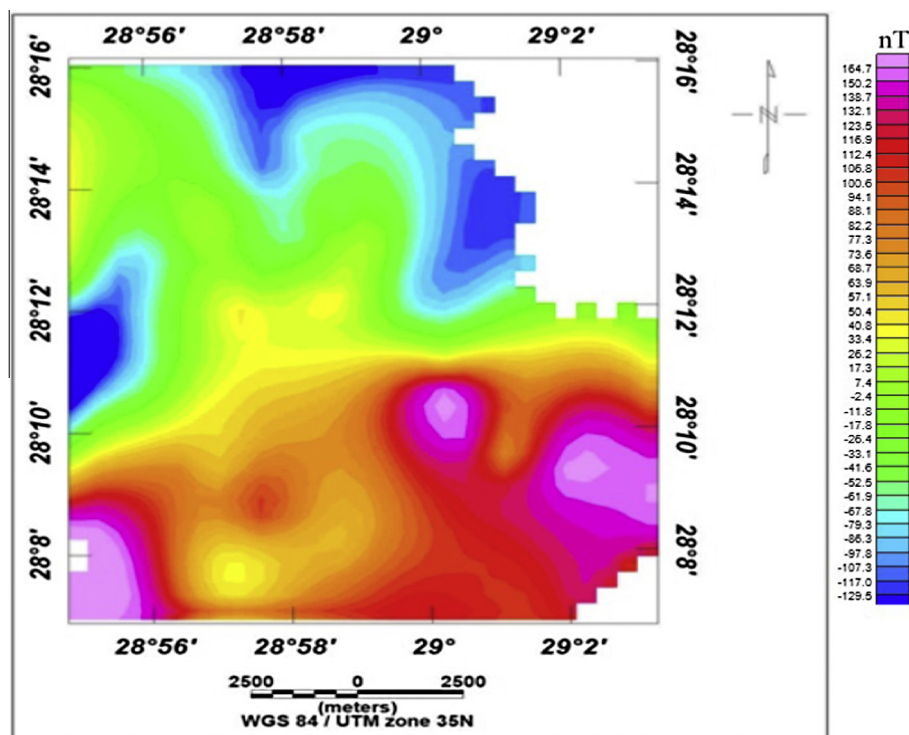


Figure 5 Total magnetic anomaly map reduced to the pole (RTP) for the study area.

characterized by long- and short-wavelength anomalies distributed throughout the study area. In general, heterogeneity and deformation of the basement rocks lead to sharp and strong magnetic signatures. The magnetic anomalies also display several dominant trends that do not occur at random but rather are generally aligned along definite and preferred axes that can be used to define magnetic provinces.

The inspection of the RTP land magnetic anomaly map of the studied area (Fig. 5) reveals that there are two lines of minor folds are developed along the east and west sides of the major anticline. Also, two fault systems are distinguished in El-Bahariya Oasis, (NE–SW) trending fault system throw ranges between 40 and 174 m, and there is another (NW–SE) trending fault system. The main highs are separated from a low by steep magnetic gradient with a shallow basement rocks. Faults and axes as well as the trends of magnetic anomalies trend in the eastern and western parts of the area. Also, the study area is characterized by intensive magnetic contour lines of high values in the south part of the study area.

There is another low magnetic anomalies located in the north part of the study area. These parts reflect very strong magnetic anomalies with steep gradients and high amplitudes at the southeastern and southwestern sides. The strong magnetic anomalies may be attributed to the occurrence of subsurface basic intrusion of high magnetic content. The most conspicuous anomalous features located in the center of the study area that has magnetic low and extends in the NW–SE and E–W directions, are represented by low magnetic anomalies of limited area extent and characterized mainly by their relatively low amplitudes, low frequencies and moderate gradient. These almost negative magnetic anomalies may be interpreted as representing structure lows or down faulted basement blocks.

2.4. Regional residual separation of the RTP land magnetic map

The separation procedures are designed to get a good resolution of the effect of the broad deeper variations “i.e. regional” from that of the sharper local ones “i.e. residual” magnetic components as two distinct magnetic maps. The residual map focuses attention on weaker features, which are obscured by strong regional effects in the original map. The separation of regional magnetic field from the residual one is achieved by applying the least square polynomials approach on the reduced to the pole magnetic data. The (high-pass) residual map of the third order (Fig. 6) is considered as the most proper and applicable for the magnetic anomalies interpretation (the resulted residuals are correlated using the correlation coefficient).

The critical analysis of the residual magnetic map of third order (Fig. 6) shows several local magnetic closures of different wavelengths, amplitudes and polarities, in which their axes are trending NE–SW and NW–SE. These closures are mainly related to the presence of local structures within the sedimentary rocks more than the basement rocks. Also we can notice that, there is a regional fault zone with NE–SW trend.

This map exhibits distinct locations of high magnetic anomalies with high amplitudes and steep gradients located at the central part of the map. In the eastern part of the area, the most striking anomalies are the N–S magnetic low of steep gradient and low frequency. The main low is separated from the high anomalies in the central part by steep magnetic gradients. These magnetic features reflect the thin sedimentary sequence and shallow depth of the basement. The magnetic anomalies across western part are characterized by different polarities (positive and negative) with N–S and E–W trends.

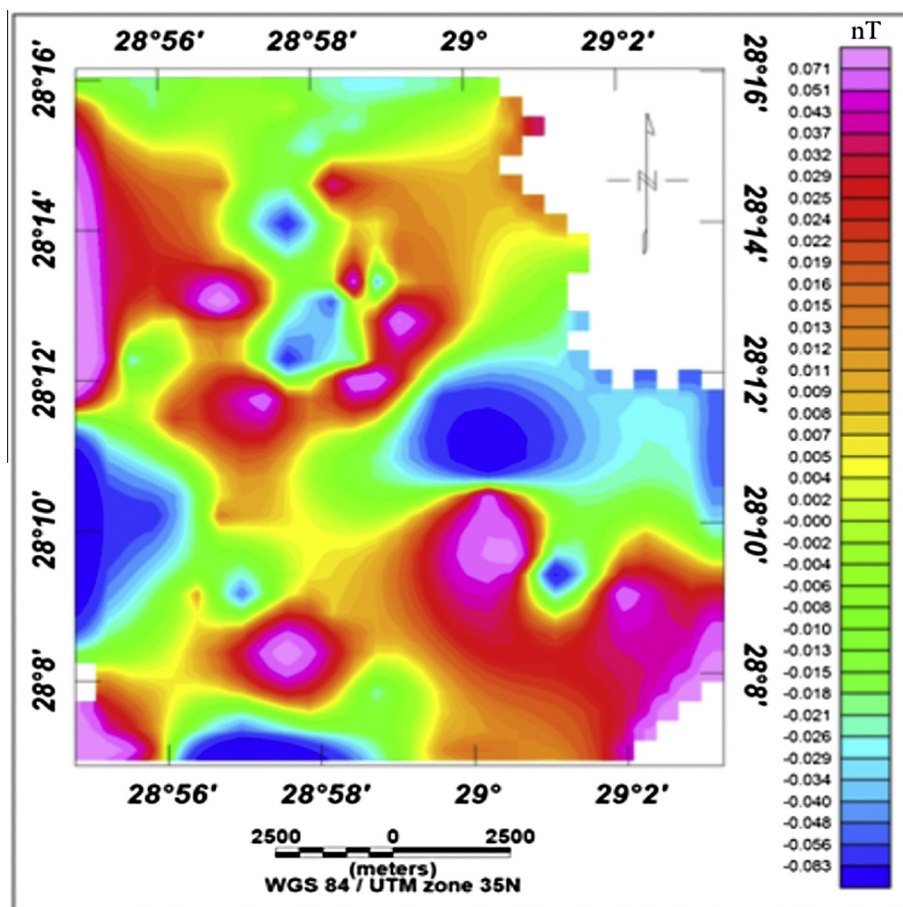


Figure 6 High-pass filtered magnetic map of the study area.

The main high anomalies are separated from the low one by steep magnetic gradient.

2.5. Horizontal gradient map

The horizontal gradient magnetic anomaly map has been prepared from the RTP land magnetic intensity anomaly map using Oasis Montaj (1998). The energy in the high frequency region, which largely consists of noises, and contribution from the near surface magnetic sources, is greatly increased. Although, the horizontal derivative is a nonlinear operation that cannot be described in terms of a linear filter, it is claimed to define a sharp contact between two rock types having different magnetization (Stanley, 1976). Such situation may occur in the faulted parts, where block displacements bring lithologies of different magnetizations to the same depth level on both sides of a fault plane. The target of applying the horizontal gradient map in this study is to compare the faulting structures deduced from the RTP land magnetic map (Fig. 5) and the filtered maps (especially the tectonic fault occurred in the El-Bahariya Oasis area, with the lineation of the horizontal gradient map). The horizontal gradient map (Fig. 7) depicts intensive NW-SE trend oriented lineation almost all over the map, except in the northwestern, and southeastern. This trend appears only in the high-pass filtered map, which reflects the shallow extent of the structures causing the anomalies.

From Fig. 7, we can see lineation with NW-SE trend especially in central part of the study area. This trend is still persisted in the RTP land magnetic map; high-pass filtered maps. It can be concluded that, study area is structurally controlled by a major axis trending NW-SE trend and extends to deep depths. Also tectonic structures resulting from the anomalies of E-W trend are extending to the intermediate depths only.

2.6. Euler deconvolution technique

The Euler deconvolution is a tool used in interpretation of the potential field methods (gravity & magnetic), for determining the depths of the contact between the sedimentary rocks and basement rocks. This technique depends on the structural index, level of the magnetic data and the sampling rate. It uses both the horizontal and vertical gradients, to calculate the location and the depth of the anomaly sources. In this investigation, the Euler deconvolution technique has been carried out on the magnetic data using Geosoft program (1998). The Euler solution at different depths is shown in Fig. 8. For interpreting contacts, faults and causative source type, for the magnetic data structural indices $SI = 1.0$ (for magnetic dykes) and $SI = 0.5$ (for magnetic fault) (Reid et al., 1990) are used. The Euler plots show somewhat more complex pattern that can be attributed to their clustering disturbance, which can

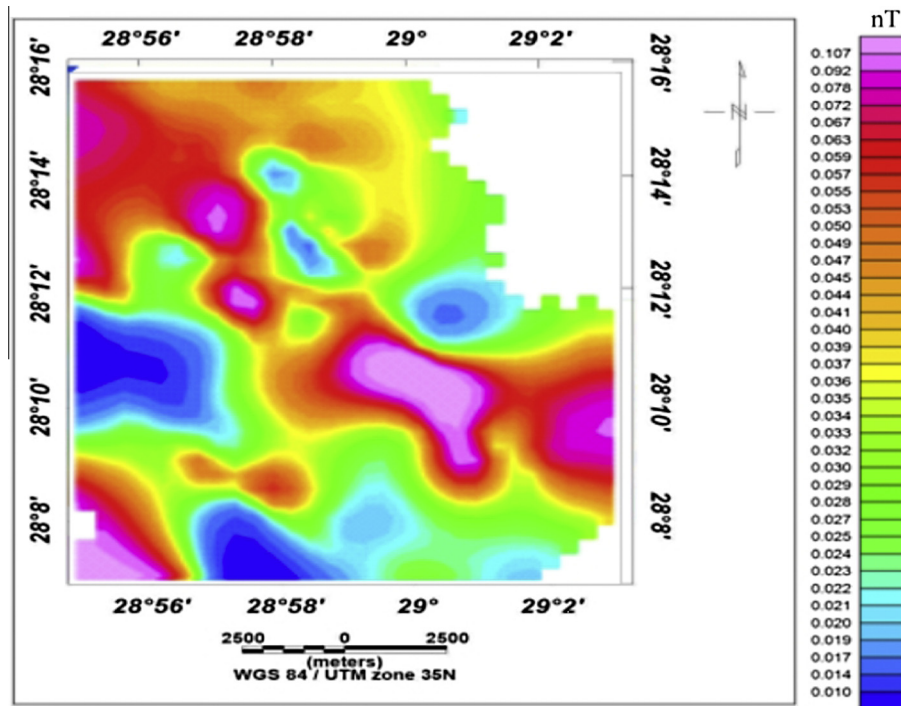


Figure 7 Horizontal gradient magnetic anomaly map of the studied area.

be interpreted as due to the dipping of the causative sources (prismatic dikes). From the Euler figure, we can notice that there are two main closures are dominated in the study area. The first one is characterized by high magnetic anomaly located in the south of the study area, while the other is characterized by low magnetic anomaly located in the north part of the study area.

3. 3-D analytical signal method

The application of the analytical signal method is recently applied as a powerful technique to evaluate the buried structures causing significant linear magnetic anomalies, such as fault zones, steps and dykes. The analytical signal map (Fig. 9) has been calculated by using the *Geosoft program* (1998). This map reveals mostly a number of elongated high anomalies trending N–S, which are characterized by increasing the small undulations in their contour lines. These anomalies are separated by a lot of local elements of high relief, small areal extensions and elongated shapes. Further, this analytical signal map could be directly used to yield the corresponding value for the expected source bodies with respect to the level of observations.

3.1. Spectral frequency analysis

Radially average power spectrum method is used to determine the depths of volcanic intrusions, depths of the basement complex and the subsurface geological structures. *Garcia and Ness (1994)* explained the spectral analysis technique in detail. In the present study, the Fast Fourier Transform (FFT) is applied on the RTP land magnetic survey data (Fig. 5) to calculate the energy spectrum. As a result, a two-dimensional power

spectrum curve is obtained (Fig. 10) and the depth estimates of the land magnetic survey anomalies, indicated that the depth to the top of the basement complex lies at 0.1 km, while the depth to the basement intrusion at depth 0.32 km, below the measuring level.

3.2. Tilt derivative filter (TDR)

Magnetic data alone give an idea about the general structure of the area. Filtering the magnetic data enhances and sharpness the anomalies and trends of the data and helps in the interpretation. Tilt Derivative filter (*TDR*) is applied to the magnetic data. The TDR and its total horizontal derivative are useful for mapping shallow basement structures and mineral exploration targets. This filter is estimated by dividing the vertical derivative by the total horizontal derivative (*Verduzco, 2004*) as below.

$$\text{TDR} = \tan^{-1}(\text{VDR}/\text{THDR}) \quad (1)$$

where *VDR* and *THDR* are first vertical and total horizontal derivatives, respectively, of the total magnetic intensity *T*.

$$\text{VDR} = dT/dz \quad (2)$$

$$\text{THDR} = \text{sqrt}\left((dT/dx)^2 + (dT/dy)^2\right) \quad (3)$$

The most advantage of the TDR is that its zero contour line is on or close to the fault/contact location. Fig. 11 shows the *TDR* map of the magnetic data with the zero contour line. TDR map enhances the magnetic trends and indicates that the major structure of the area is N–S direction. Also there are some other trends in the area, (NE–SW) and (NW–SE) directions. So, we can notice that there are two fault systems are distinguished in Bahariya Oasis, (NE–SW) trending fault system, another (NW–SE) trending fault system.

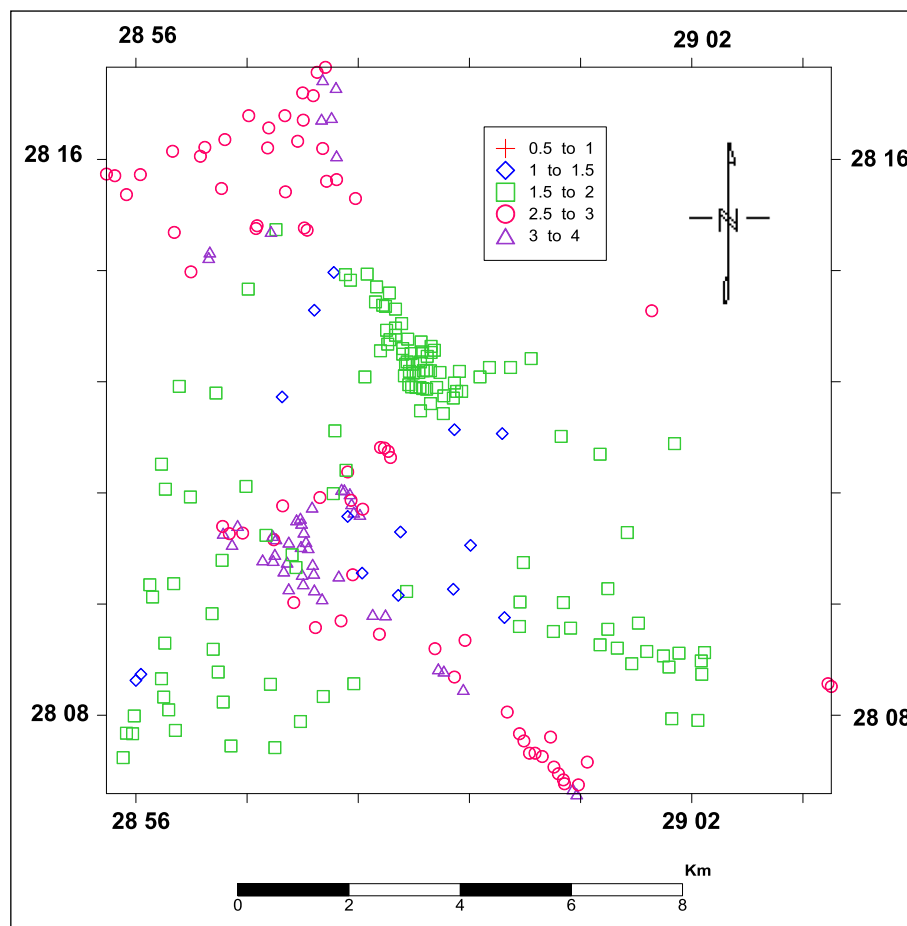


Figure 8 Euler deconvolution for magnetic map of the studied area.

The TDR theory indicates that the zero contour line will be located at or very close to the fault/contact. Tracing the zero contour line of the TDR map delineates the subsurface structure of the area and thus drawing the faults that characterize the area. It indicates that the main trend of the area is the E–W direction.

3.3. Geothermal analysis

Knowledge of temperature within the earth is essential for the proper understanding of many properties and processes. The temperature of the earth increases with depth, but the temperature field is mostly not a simple function (Chapman and pollak, 1977). Geothermal methods are suitable not only for exploration of geothermal energy sources, but also for detecting of subsurface bodies with different thermal conductivity and subsurface bodies representing (positive and negative) heat sources.

Thermal or hot springs are surface manifestations of the heat loss from the earth, and are commonly associated with geothermal area. El-Ramely (1969) compiled a list of springs in Egypt which are located along the shores of the Gulf of Suez and Western Desert area (El-Bahariya, Siwa and El-Farafra Oases). These springs properly owe their existence to tectonic movements. Said, 1962 however, suggested that they are

related to hydrothermal activities accompanying the magmatic activity during the Oligocene time.

3.4. Main earth temperature contour map

Soil temperature varies from month to month as a function of incident solar radiation, rainfall, seasonal swings in overlying air temperature, local vegetation cover, type of soil, and depth in the earth. Due to the much higher heat capacity of soil relative to air, the thermal insulation is provided by vegetation and surface soil layers. In the present work, Geo-temperature survey has been carried out using the device of thermophysical properties (ISOMET-104) for measuring subsurface temperature at 50 cm below. Geo-temperature contour map in El-Bahariya oasis (Fig. 12) is relatively low in the northwestern side (less than 15 °C), and higher in the eastern side (more than 40 °C). These features resulted not only from special geological conditions, but also from regional geothermal background. On this map of estimated geo-temperature, some areas of temperature ranging from 15 to 50 °C as shown in Fig. 12 are laying around thermal springs in the study area. Besides these high temperature zones affected by thermal springs (El Bawiti and El Harra hot springs), the heat seems to be related to hydrothermal activities and accompanies the magmatic activity during the Oligocene age.

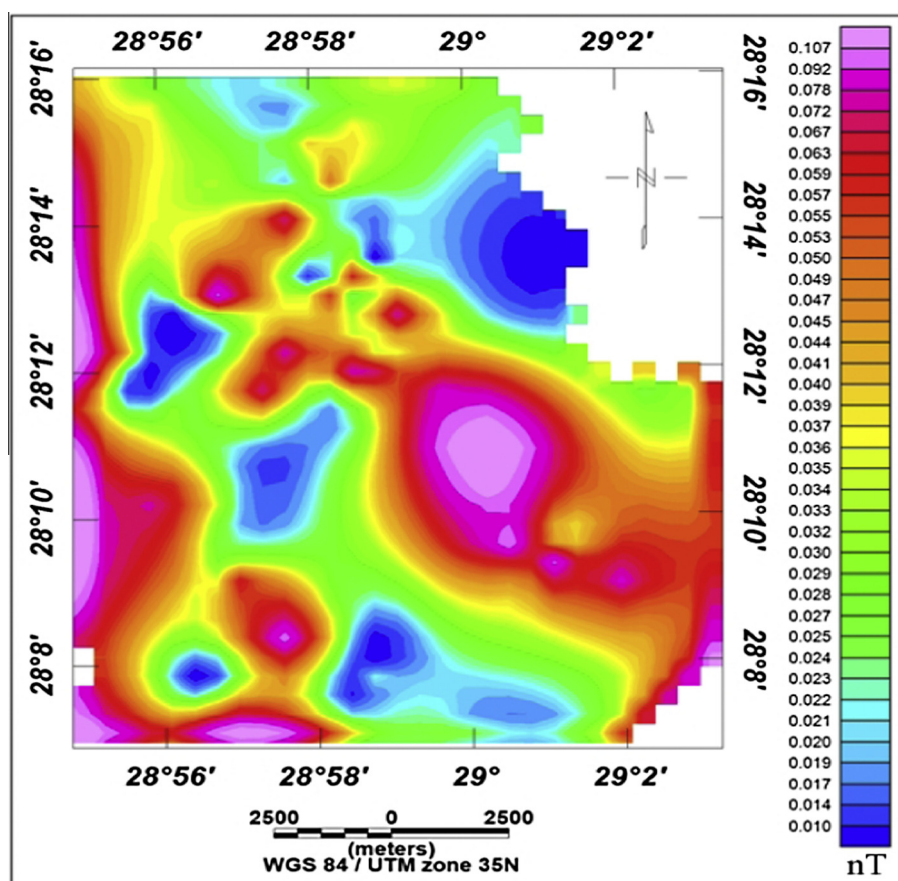


Figure 9 Analytical signal map of the studied area.

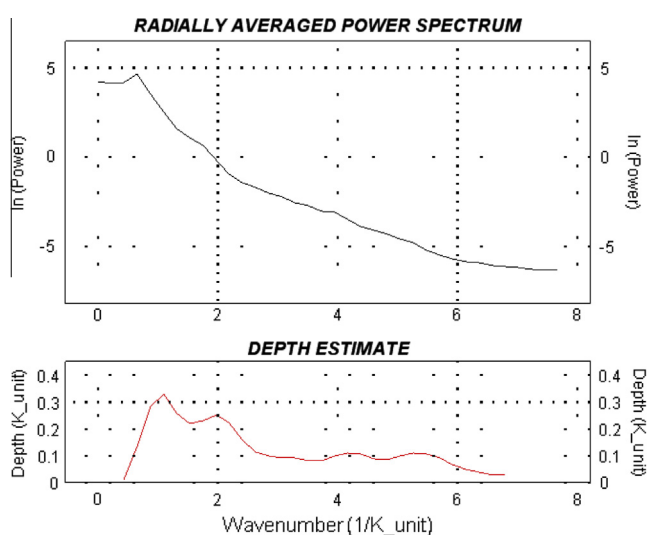


Figure 10 Two-dimensional local power spectrum of the RTP land magnetic map of study area.

3.5. Laboratory measurements of thermo-physical properties

Twenty-four geological rock samples (15-sandstone & 9-limestone) have been collected from some places in El-Bahariya Oasis. Thermo-physical properties of these rock samples are measured through ISOMET instrument.

3.6. Thermo-physical properties instruments

The device of thermo-physical properties is ISOMET model 104, Bratislava, Slovakia. It is a microprocessor controlled portable device for direct measurement of thermo-physical properties of various solid and liquid materials such as:

- Thermal conductivity ($\text{W m}^{-1} \text{K}^{-1}$);
- Volume conductivity ($\text{J m}^{-3} \text{K}^{-1}$);
- Thermal diffusivity ($\text{m}^2 \text{s}^{-1}$);
- Temperature degrees ($^{\circ}\text{C}$);

where W = watt, K = Kelvin, J = joule, m = meter, and S = second.

This device may be equipped by various exchangeable probes, needle probes for porous or soft materials, surface probes for hard materials, and measuring cells for liquids. Each probe has built-in memory with its calibration data ensuring great variability of device without affecting measurement accuracy.

3.6.1. The relationship between the thermal conductivity and temperature values for both sandstone and limestone rock samples

Figs. 13 and 14 show the relationship between thermal conductivity and temperature at different places in Bahariya Oasis. From these figures, we can notice that the thermal conductivity of sandstone and limestone differs from place to another.

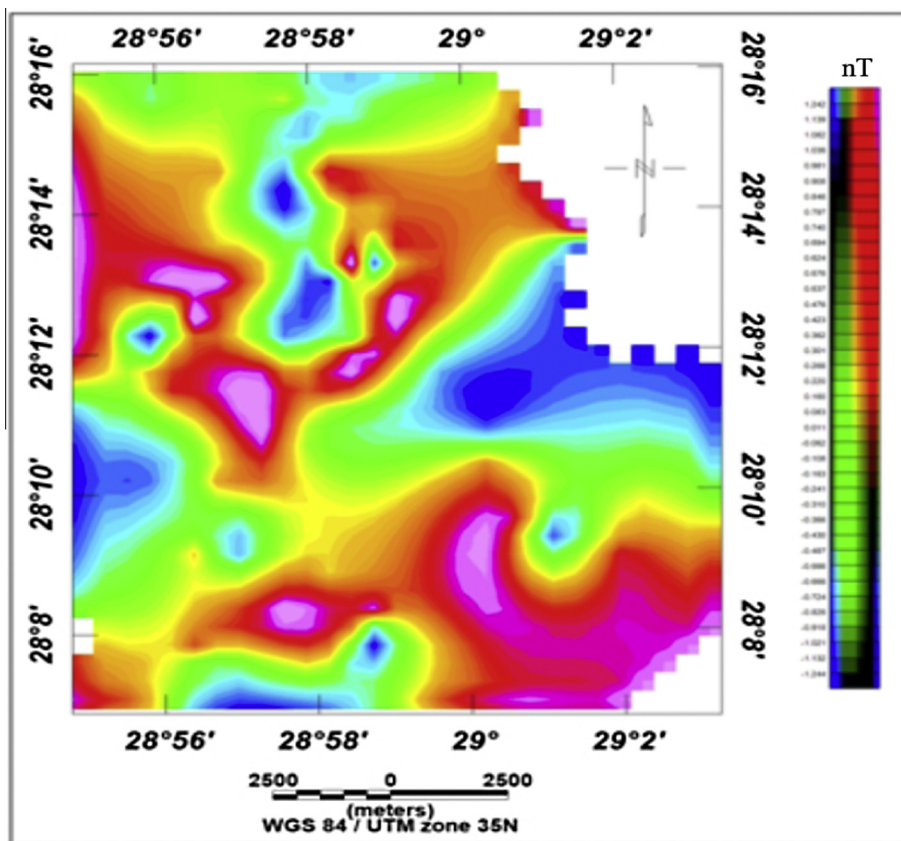


Figure 11 Tilt derivative filter (TDR) of the magnetic map.

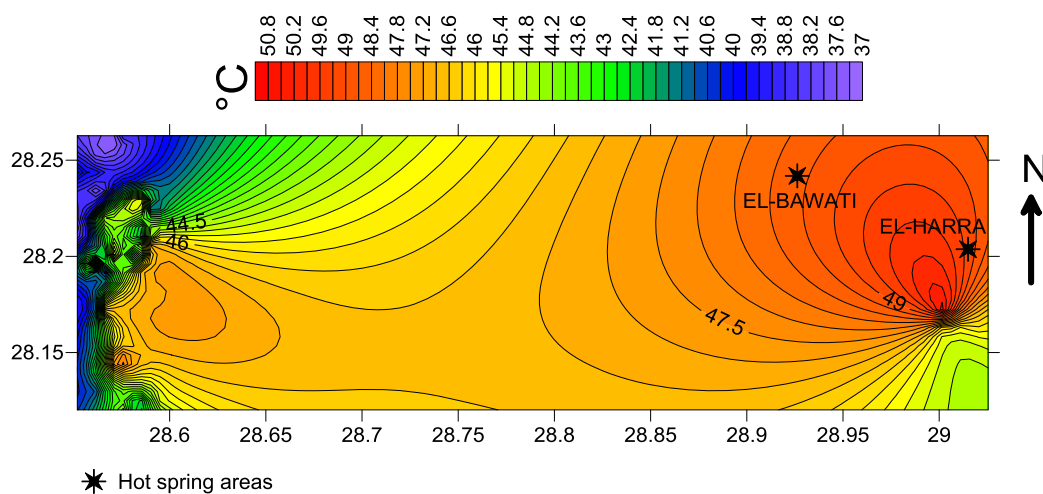


Figure 12 Geo-temperature contour map at 0.5 m depth around thermal areas in El-Bahariya Oasis.

The thermal conductivity values for both sandstone and limestone rock samples (measured in the same room temperature) decrease substantially with increasing temperature values. The great majority of the thermal conductivity of sandstone values ranges between 0.36 and $0.42 \text{ W m}^{-1} \text{ K}^{-1}$, while the average values of limestone are between 0.31 and $0.47 \text{ W m}^{-1} \text{ K}^{-1}$.

3.6.2. Relation between the volume heat capacity and temperature values for sandstone rock samples

The volumetric heat capacity of the rock samples shows different values from place to another. The volumetric heat capacity value that was measured at ambient condition ranges from $0.50 \text{ E}+6$ to $0.70 \text{ E}+6 \text{ J m}^{-3} \text{ K}^{-1}$ as shown in Fig. 15. It increases with increasing temperature values. The maximum

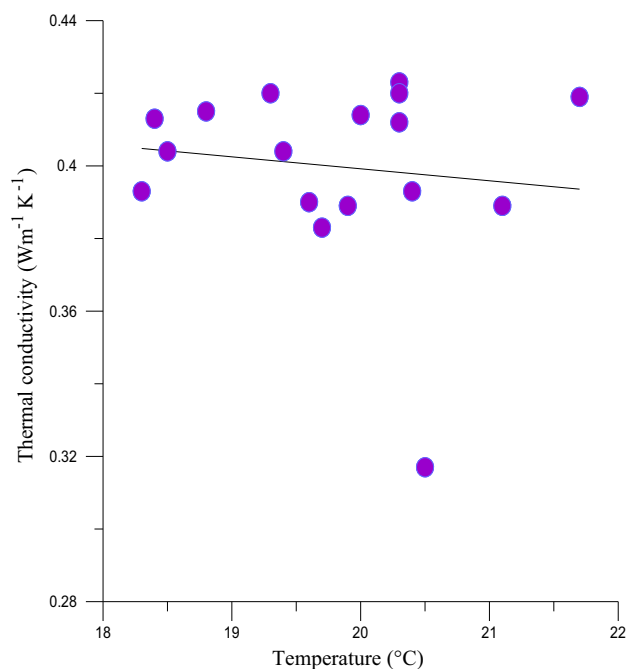


Figure 13 Variations of the thermal conductivity with temperature for the sandstone rock samples from El-Bahariya Oasis hot spring.

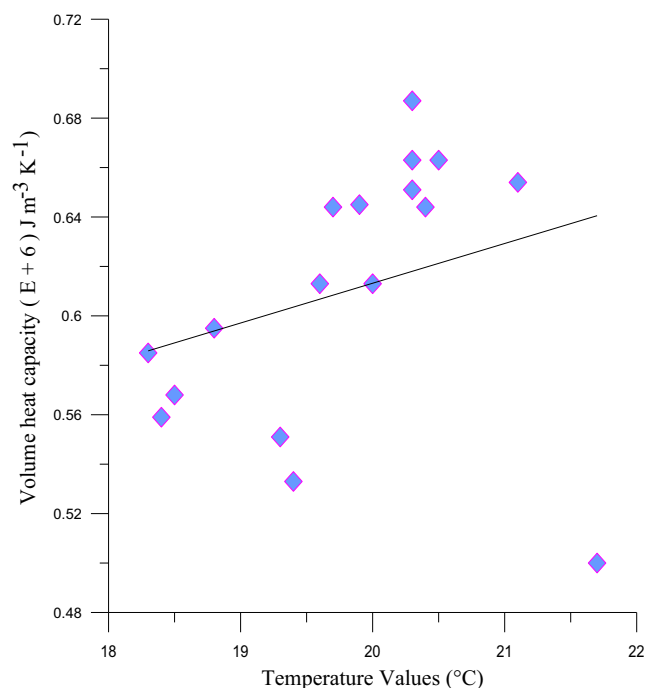


Figure 15 Variations of the volume heat capacity with temperature values for sandstone rock samples from El-Bahariya Oasis.

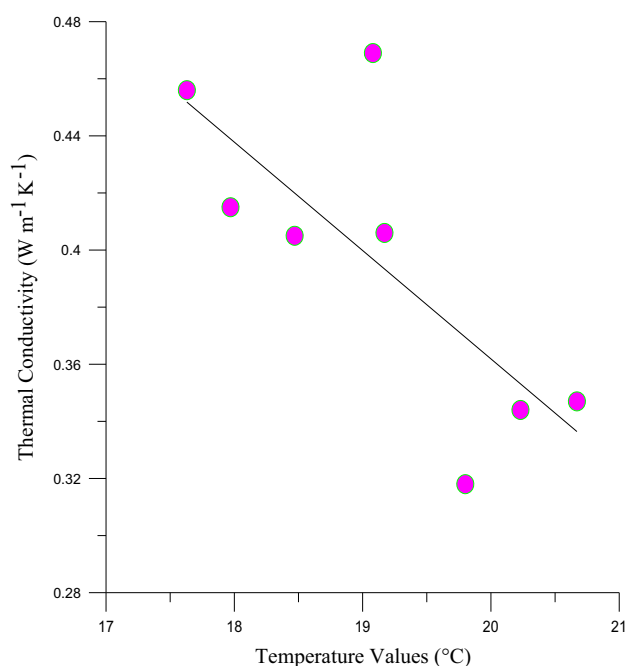


Figure 14 Variations of the thermal conductivity with temperature for the limestone rock samples from El-Bahariya Oasis hot spring.

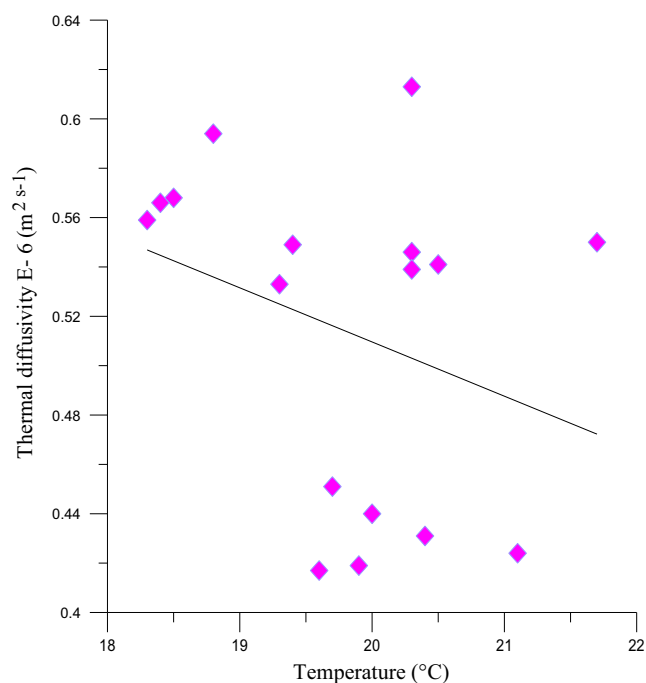


Figure 16 Variations of the thermal diffusivity with temperature values for sandstone rock samples from El-Bahariya Oasis.

value was around $0.75 \text{ E} + 6 \text{ J m}^{-3} \text{K}^{-1}$ as shown as in Fig. 15. These lowest values may be due to the effect of weathering conditions and the rock samples are not pure and have different minerals.

We notice that both the thermal conductivity and thermal diffusivity values for sandstone and limestone rock samples decrease with increasing temperature values, while the volume heat capacity values increase with increasing temperature values.

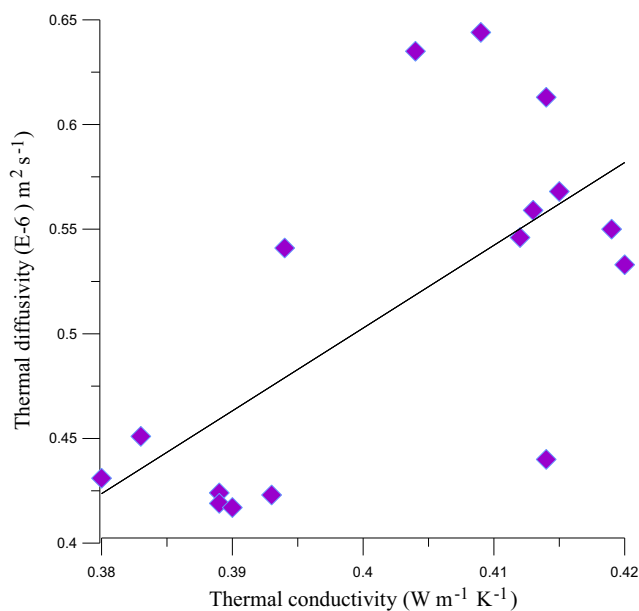


Figure 17 The relation between the thermal diffusivity and thermal conductivity values for sandstone rock samples from El Bahariya Oasis hot spring.

3.6.3. Relation between thermal diffusivity values and temperature values for sandstone rock samples

The values of thermal diffusivity for rock sandstone samples decrease with increasing the temperature values as shown in Fig. 16. The average values of sandstone rock samples range from, 0.42 E-6 to 0.62 E-6 m² s⁻¹.

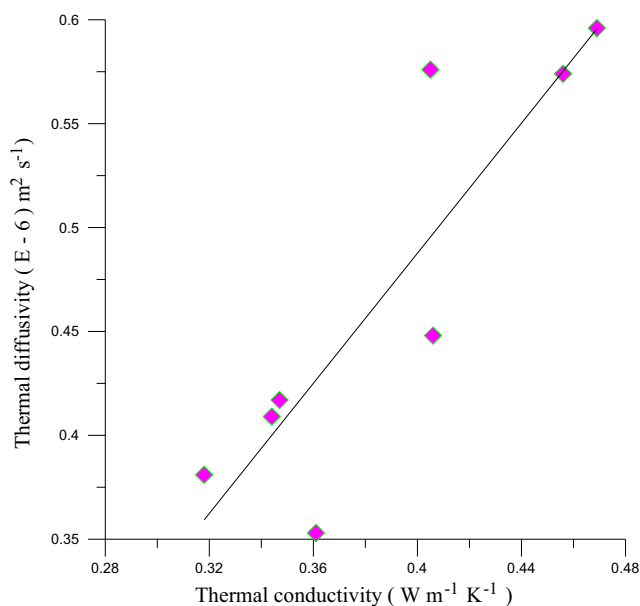


Figure 18 The relation between the thermal diffusivity and thermal conductivity values for limestone rock samples from El Bahariya Oasis hot spring.

3.6.4. Relationship between the thermal conductivity and the thermal diffusivity for both sandstone and limestone rock samples

There are direct relation between the thermal conductivity and the thermal diffusivity values for both sandstone and limestone rock samples (Figs. 17 and 18). It could be noticed that there is general decrease in thermal conductivity values with increasing the thermal diffusivity values.

3.6.5. Relation between the thermal conductivity and the volume heat capacity values for limestone rock samples

It could be noticed that there is direct relation between the thermal conductivity and the volume heat capacity values for limestone rock samples (Fig. 19). This means that, the limestone rock samples have a high values of the thermal conductivity at high values of the volume heat capacity.

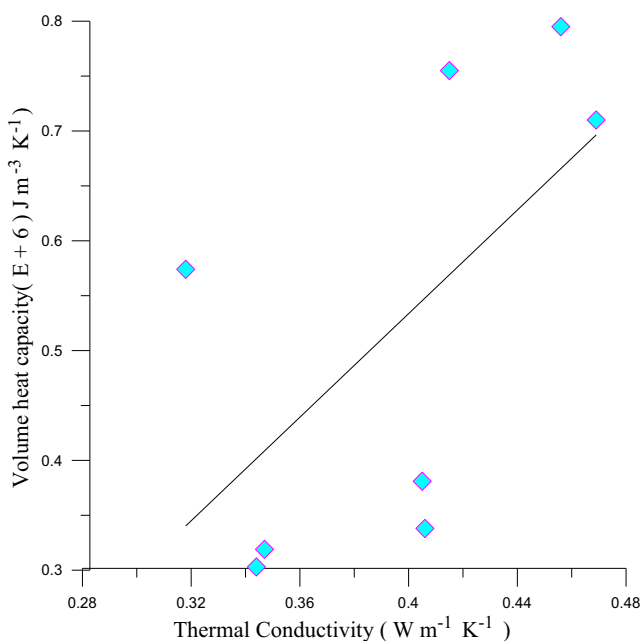


Figure 19 The relation between the thermal conductivity and the volume heat capacity for limestone samples from El Bahariya Oasis hot.

4. Discussion and conclusions

The integration of geophysical data, magnetic and geothermal, can reduce the ambiguity of geological interpretations in various geological settings. Our interpreted magnetic and geothermal data of the El-Bahariya Oasis area have revealed new information and improved the knowledge about the internal structure beneath this area. Close examination of the different anomalies through the RTP magnetic maps reveals that, the study area is characterized by intensive positive magnetic anomalies with different amplitudes. These anomalies may be attributed to the occurrence of subsurface basic intrusions of high magnetic content at different depths. The RTP land magnetic map (Fig. 5) revealed that there are two lines of minor folds which are developed along the east and west sides of the major anticline. Also, two fault systems are distinguished in Bahariya Oasis, (NE-SW) trending fault system, another (NW-SE) trending fault system. The differences in magnetic

relief between each two adjacent magnetic highs and lows suggest a comparable variation of composition of the subsurface rocks. Filtering the magnetic maps serves to improve the understanding of the geological configuration of the basement and the overlying sedimentary cover. Therefore, the filters used are grouped into three categories, namely high and low – pass filters. The analysis of filtered maps indicates that, the high pass magnetic filtered map shows that, the area is varying into two portions, the eastern and western lows with negative anomalies and the northwestern and southeastern parts are high positive one; these are separated by steep gradients oriented NW–SE and NE–SW. This reflects the deep extension of the structures causing the anomalies.

The results obtained from Euler technique showed that there are two main closures are dominated in the study area. The first one is characterized by high magnetic anomaly located in the south of the study area, while the other is characterized by low magnetic anomaly located in the north part of the study area. Depth estimations were conducted by application of the power spectrum. The results refer that, the average calculated depth ranges between 0.1 km and 0.2 km, while the depth to the basement intrusion at depth 0.4 km, below the measuring level. The TDR theory indicates that the zero contour line will be located at or very close to the fault/contact. Tracing the zero contour line of the TDR map delineates the subsurface structure of the area and thus drawing the faults that characterize the area. It indicates that the main trend of the area is the E–W direction.

Geothermal studies in some places in El-Bahariya Oasis have been carried out using the device of thermo-physical properties (Isomet-104) for measuring the subsurface temperature contour map (50 m below the earth's surface). The obtained map illustrates that there are good geothermal regions have hot groundwater reservoir that is located in the eastern side of the study area. The measurements of geothermal properties of some rock samples (sandstone and limestone) such as thermal conductivity, thermal diffusivity, volume capacity and thermal values give us an indication about the geothermal of rocks in the subsurface. Also, they give an idea about the heat flow and the increasing of the energy and physical properties of the predominant subsurface rocks in the study area.

Acknowledgments

This paper has been supported by the Egyptian Science and Technology Development Fund Program STDF through the research project: “Geomagnetic Survey & Detailed Geomagnetic Measurements within the Egyptian Territory” ID 1275.

References

- Chapman, D.S., Pollak, H.N., 1977. Regional Geothermic and Lithospheric Thickness. *Geology*, 5, Boulder Col., pp. 265–268.
- El-Atre, H.A., Moustafa, A.R., 1980. Utilization of orbital imagery and conventional aerial photography in the delineation of the regional lineation pattern of the central western desert of Egypt with a particular emphasis on the Bahariya region. In: *The Geology of Libya*, vol. 3. Academic Press, New York, pp. 933–953.
- El-Ramely, I.M., 1969. Recent review of investigation on the thermal and mineral springs in the U.R.A. In: XXII International Geological Congress, 19, pp. 201–213.
- El Sisi, Z., Hassouba, M., Oldani, M., Dolson, J., 2002. The geology of Bahariya Oasis in the Western Desert of Egypt and its archeological heritage. In: *Cairo 2002 International Conference and Exhibition*.
- Garcia, J.G., Ness, G.E., 1994. Inversion of the power spectrum from magnetic anomalies. *Geophysics* 59, 391–400.
- Hvidt, M., 1999. *Water Resource Planning in Egypt. The Middle Eastern Environment*, Published by St. Malo Press. Odense University, Denmark. ISBN 1 898565 031.
- Korany, E.A., 1981. Analysis and evaluation of step-draw down and recovery tests, Bahariya mines area, Western Desert, Egypt. In: 6th Inter. Cong. Statist. Soc. Research, pp. 217–240.
- Korany, E.A., 1984. *Geochemical Functions of Groundwater Flow in the Bahariya Oasis, Western Desert, Egypt*.
- Oasis Montaj, 1998. *Geosoft Mapping and Application System Inc., Suit 500, Richmond St. West Toronto, On Canada N5S1V6*.
- Reid, A.B., Allsop, J.M., Granser, H., Millett, A.J., Somerton, I.W., 1990. Magnetic interpretation in three dimensions using Euler deconvolution. *Geophysics* 55, 80–90.
- Said, R., 1962. *The Geology of Egypt*. Elsevier, Amsterdam, 377p.
- Salem, M., 1987. *Pedological Characteristics of Bahariya Oasis Soils*. Ph. D. Thesis, Faculty of Agriculture, Ain Shams University, Egypt.
- Stanley, S.M., 1976. Simplified magnetic interpretation of the geologic contact and thin dike. *Geophysics* 42, 1236–1240.
- Verduzco, B., 2004. New insights into magnetic derivatives for structural mapping. *Lead. Edge* 23, 116–119.